Kinematics of the line of sight angle and image-center deviation of the observatory on the mobile vehicle in terms of affecting speed and attitude

Vu Quoc Huy*

Institute of Automation, Academy of Military Science and Technology, 89B Ly Nam De, Hoan Kiem, Hanoi, Vietnam.

*Corresponding author: maihuyvu@gmail.com

Received 08 Jan. 2026; Revised 11 May 2026; Accepted 10 Aug. 2026; Published 25 Aug. 2026.

DOI: https://doi.org/10.54939/1859-1043.j.mst.113.2026.38-47

ABSTRACT

This paper analyzes the formation of line-of-sight (LOS) interference in EO/IR systems due to carrier movement using a three-coordinate kinematic model and pinhole projection. From the given formulas, the paper clarifies the influence of horizontal velocity $v_\perp$ and angular deviation δ on LOS rotation speed and pixel drift. Simulation results show that interference is minimal when the carrier is oriented directly toward the target, but increases significantly when a horizontal velocity component is present, especially during phase changes or maintaining the target at a camera-off position. Based on the obtained kinematic analysis, the paper suggests future LOS stabilization systems. The results obtained provide a useful quantitative basis for the design, operation, and optimization of EO/IR tracking systems under mobile carrier conditions.

Keywords: Line-of-sight dynamics; Electro-optical stabilization; Geometric kinematics; Image-plane deviation; Moving platforms.

1. INTRODUCTION

Electro-optical/infrared (EO/IR) observation systems installed on mobile vessels at sea are increasingly playing an important role in monitoring, surveillance, and tracking targets at long distances. However, the performance of these systems is significantly affected by the movement of the carrier base. When the ship is affected by waves, wind, or maneuvers, the linear and angular velocity components of the carrier base will be transmitted directly to the line-of-sight (LOS), causing angular deviation and shifting of pixels on the sensor. This phenomenon has been clearly observed in classic studies on electro-optical stabilization platforms on ships and vehicles, showing a close relationship between base movement and LOS interference [1-4, 6, 8].

In many research and practical applications, the problem of EO/IR image stabilization is often solved through a two-axis mechanical structure (pan-tilt/gimbal) combined with feedback controllers to suppress noise caused by the angular velocity of the carrier [6, 7, 9]. Some recent studies have extended the control structure by adding a feedforward compensation branch from the inertial signal (IMU/INS), thereby improving the LOS stabilization quality under conditions of a highly mobile carrier [11, 12]. Such stabilization architectures are also consistent with classical multivariable feedback and disturbance-rejection frameworks discussed in [5]. However, in most of these approaches, LOS noise is still often modeled as an extraneous signal or unstructured noise, without fully analyzing its formation nature from the geometric-kinematic relationship between the target, camera, and carrier.

In fact, even when the absolute speed of the vehicle is not large, the existence of a horizontal velocity component relative to the line of sight, which often appears in the turning phases or when the target is off-axis of the camera, can still cause significant LOS rotation speed, leading to rapid pixel slippage on the image plane. These phenomena have been mentioned sporadically in studies on LOS velocity modeling and inertial stabilization error analysis [8, 10], but often lack a unified dynamic model directly linking background velocity, viewing posture, and pixel misalignment on the sensor. Therefore, building a clearly structured LOS dynamic model, derived from rotations in

SO(3) and directly linked to the camera's pinhole projection model, is necessary to clarify the mechanism of LOS noise formation as well as quantitatively assess the influence of background velocity components. Such a geometric-kinematic approach has been confirmed as an important foundation for designing more effective image-tracking and LOS stabilization controllers under mobile carrier conditions and turbulent sea environments [11, 12, 14]. Similar geometric modeling concepts for pan-tilt camera tracking systems have also been investigated in underwater and mobile vision platforms [13].

Based on this requirement, this paper focuses on building and analyzing the LOS angle kinematic model of the EO/IR system mounted on a mobile vehicle, considering the influence of carrier velocity and attitude through three coordinate systems: Earth-Body-Camera. The model is directly linked to image projection to clarify the relationship between LOS angle deviation and pixel displacement on the sensor. The results obtained provide a mathematical and experimental basis for evaluating the allowable maneuver limit, and guide the design of feedforward compensation control and optimal control solutions to improve the LOS stabilization performance of the EO/IR system under actual combat conditions. It should be emphasized that the Earth-Body-Camera coordinate representation and DCM-based rotational modeling are classical approaches in geometric kinematics. The contribution of this work is therefore not the introduction of a new DCM formulation itself, but rather the explicit quantitative linkage between carrier horizontal velocity, LOS angular-rate disturbance, and image-plane pixel drift under practical EO/IR operating conditions.

2. THEORETICAL FOUNDATION OF LOS KINEMATICS

2.1. Coordinate systems and associated rotations

Consider three coordinate systems: i) Σ_E (Earth-fixed) is the frame of reference attached to the ground, ii) Σ_B (Body) is the coordinate system attached to the vehicle, iii) Σ_C (Camera) is the coordinate system attached to the observatory. R_{XY} is the rotation matrix of vectors from Y to X, that is $v_X = R_{XY} v_Y$. The rotation from $\Sigma_E \to \Sigma_B$ is described by the Euler rotation sequence: $R_z(\psi)R_y$ $(\theta)R_x(\phi)$, which gives the orientation matrix from Earth to the vehicle body, with rotation angles roll (ϕ), pitch (θ), and yaw (ψ).

Denoting: R_{XY}: The rotation matrix transforming coordinates from frame Y to frame X; $v_\perp$: Velocity perpendicular to LOS; ω_{LOS}: LOS angular rate; u, v: Image-plane coordinates; f_x, f_y: Camera focal lengths; Z: Depth; S: Pixel/radian scaling factor; r_c: Line of sight (LOS) vector in the camera frame; r_t and r_v: Target and platform positions on Earth; and α, β: Rotation angles of the pan and tilt axes, respectively, with the condition that the pan rotates around the z_B axis and tilt rotates around the x_C axis. Defining $\cos x \overset{\text{def}}{=} cx, \sin x \overset{\text{def}}{=} sx$, we have:

$$R_{BE} = R_x(\phi)R_y(\theta)R_z(\psi) = \begin{bmatrix} c\theta c\psi & c\theta s\psi s & -s\theta \\ s\phi s\theta c\psi - c\phi s\psi c & s\theta s\psi + c\phi c\psi & s\phi c\theta \\ \phi s\theta c\psi + s\phi s\psi & \phi c\phi s\theta s\psi - s\phi c\psi & c\phi c\theta \end{bmatrix} \tag{1}$$

Similarly, the orientation matrix R_{CB} between the camera and the vehicle body (Pan-Tilt) is:

$$R_{CB} = R_x(\beta)R_z(\alpha) \tag{2}$$

The line of sight (LOS) vector in the camera frame is:

$$r_c = R_{CB}R_{BE}(r_t - r_v) = R_{CB}R_{BE}P_{rel}, \qquad P_{rel} = (r_t - r_v) \tag{3}$$

The notation $[\omega]_\times$ represents the skew matrix of the angular velocity vector ω:

$$\omega = \begin{bmatrix} \omega_x & \omega_y & \omega_z \end{bmatrix}^T$$

Skew matrices are uniquely defined by the relation: $[\omega]_\times a = \omega \times a,\ \forall a \in R^3$

By definition, the explicit form of $[\omega]_\times$ is:

$$[\omega]_\times = \begin{bmatrix} 0 & -\omega_z & \omega_y \\ \omega_z & 0 & -\omega_x \\ -\omega_y & \omega_x & 0 \end{bmatrix} \quad (4)$$

This matrix satisfies the skew-symmetric property $[\omega]_\times^T = -[\omega]_\times$ and is the matrix representation of the cross product in 3-dimensional space. The total angular velocity of the camera frame (relative to the inert frame) is represented by ω_c, shown in the camera frame.

2.2. Kinematics of LOS angle

The rotations between coordinate systems are described by cosine orientation matrix (DCM). For example, from Σ_E sang Σ_B is described by the matrix R_{BE} which satisfies property (5).

$$R_{BE}^T R_{BE} = I,\ \det(R_{BE}) = 1 \quad (5)$$

Therefore, all rotations belonging to the SO(3) group preserve the standard and angle, ensuring the geometric consistency of the model. When considering successive systems $\Sigma_E - \Sigma_B - \Sigma_C$, the matrix product $R_{CE} = R_{CB} R_{BE}$ still belongs to SO(3), so the LOS model always preserves its geometry. Let ω_{CB} be the angular velocity of the camera frame relative to the body (pan-tilt) but represented in the camera frame. To describe the time variation of the LOS direction, we use the basic differential relationship of DCM:

$$\dot{R}_{CB} q = \omega_{cb}^{(c)} \times (R_{CB} q), \forall q \quad (6)$$

In which the derivative of DCM follows the differential relation. This relation ensures that when the vehicle has angular velocity ω, the derivative of the rotation matrix still belongs to the SO(3) space. Take the derivative of (3):

$$\dot{r}_c = \dot{R}_{CB} R_{BE} P_{rel} + R_{CB} \dot{R}_{BE} P_{rel} + R_{CB} R_{BE} \dot{P}_{rel} \quad (7)$$

On the other hand, we have:

$$R_{CB}(R_{BE} P_{rel}) = \omega_{cb}^{(c)} \times (R_{CB} R_{BE} P_{rel}) = \omega_{cb}^{(c)} \times r_c \quad (8)$$

Let ω_b be the angular velocity of the body as represented in the body frame:

$$\dot{R}_{BE} P_{rel} = \omega_b^{(b)} \times (R_{BE} P_{rel}) \quad (9)$$

Apply R_{CB} to the result and use the property $R_{CB}(u \times v) = (R_{CB}\, u) \times (R_{CB}\, v)$:

$$R_{CB} \dot{R}_{BE} P_{rel} = R_{CB}(\omega_b^{(b)} \times (R_{BE} P_{rel})) = (R_{CB} \omega_b^{(b)}) \times (R_{CB} R_{BE} P_{rel}) \quad (10)$$

Let $\omega_b^{(c)} \equiv R_{CB} \omega_b^{(b)} = R_{CB} R_{BE} \omega_b$ - This is the angular velocity of the body as represented in the camera frame. Then:

$$R_{CB} \dot{R}_{BE} P_{rel} = \omega_b^{(c)} \times r_c \quad (11)$$

Combine them, and we have:

$$\dot{r}_c = \left(\omega_{cb}^{(c)} + \omega_b^{(c)}\right) \times r_c + R_{CB} R_{BE} \dot{P}_{rel} \quad (12)$$

Define the total angular velocity of the camera within a camera frame:

$$\omega_c = \omega_{cb}^{(c)} + \omega_b^{(c)} = \omega_{cb}^{(c)} + R_{CB} R_{BE} \omega_b \quad (13)$$

So we have (14): $\dot{r}_c = \omega_c \times r_c + R_{CB} R_{BE} \dot{P}_{rel}$ (14)

Considering the objective of remaining still, $v_t = \dot{r}_t = 0$, we have:

$$\dot{r}_c = \omega_c \times r_c - R_{CB} R_{BE} \dot{r}_v \quad (15)$$

Separate $\dot{r}_v$ into two components: The component of movement in the same or opposite direction as the LOS ($v_{||}$) and the component of movement perpendicular to the LOS ($v_\perp$). With $\hat{n}_e$ being the unit vector perpendicular to the LOS line of sight, and $\hat{r}_e$ being the unit vector of the

LOS line of sight in the Earth system, we have:

$$\dot{r}_v = v_{||}\hat{r}_e + v_{\perp}\hat{n}_e$$

Similarly, switch to the camera frame:

$$R_{CB}R_{BE}\dot{r}_v = v_{||}\hat{r}_c + v_{\perp}\hat{n}_c \tag{16}$$

The component $v_{||}\hat{r}_c$ changes the depth (z) but does not rotate the direction. The component $v_{\perp}$ $\hat{n}_c$ causes LOS rotation. If only the angle part is considered:

$$\dot{r}_c \approx \omega_c \times r_c - v_{\perp}\hat{n}_c \tag{17}$$

Taking the second derivative from (14) with respect to time, we get:

$$\ddot{r}_c = \dot{\omega}_c \times r_c + \omega_c \times \dot{r}_c + \frac{d}{dt}(R_{CB}R_{BE}(\dot{r}_t - \dot{r}_v)) \tag{18}$$

In the case where the target remains stationary ($\dot{r}_t = 0$) and if we assume $v_{\perp}$ and ω_c change little over small intervals (to see the structure of the terms), we have:

$$\ddot{r}_c = \dot{\omega}_c \times r_c + \omega_c \times (\omega_c \times r_c) - \frac{d}{dt}(R_{CB}R_{BE}\dot{r}_v) \tag{19}$$

Extending $\omega_c \times (\omega_c \times r_c)$ in the familiar triple-product identity form in rotational kinematics, describing the centrifugal component and the component along the axis of rotation, we have (20).

$$\omega_c \times (\omega_c \times r_c) = -(\omega_c\omega_c)r_c + (\omega_c^T r_c)\omega_c \tag{20}$$

If we continue the expansion and assume $\dot{r}_v$ is constant (or small), then the translation part decomposes into $-\dot{v}_{\perp}\hat{n}_c - v_{\perp}\dot{\hat{n}}_c$ with $\dot{\hat{n}}_c \approx \omega_c \times \hat{n}_c$. Therefore, we can achieve:

$$\ddot{r}_C = \dot{\omega}_c \times r_c + \omega_c \times (\omega_c \times r_c) - 2\omega_c \times (v_{\perp}\hat{n}_c) - \dot{v}_{\perp}\hat{n}_c + (small\ terms) \tag{21}$$

The components that appear can be interpreted as follows:

Term 1: $\dot{\omega}_c \times r_c$ represents the change in angular acceleration.

Term 2: $\omega_c \times (\omega_c \times r_c)$ represents the centrifugal velocity, which appears when the frame rotates with ω_c.

Term 3: $-2\omega_c \times (v_{\perp}\hat{n}_c)$ is the Coriolis-like (when there is both rotation and a horizontal translational component).

Term 4: $-\dot{v}_{\perp}\hat{n}_c$: when the horizontal velocity changes.

From $r_c = [x_c, y_c, z_c]^T$ the azimuth and elevation angles are defined:

$$\alpha = \text{atan}(y_c/x_c),\ \ \beta = \text{atan}\left(\frac{z_c}{\sqrt{x_c^2 + y_c^2}}\right) \tag{22}$$

Derivatives of these angles with respect to time:

$$\dot{\alpha} = \frac{x_c\dot{y}_c - y_c\dot{x}_c}{x_c^2 + y_c^2} \tag{23}$$

$$\begin{aligned}\dot{\beta} &= \left(\dot{z}_c\sqrt{x_c^2 + y_c^2} - z_c\frac{x_c\dot{x}_c + y_c\dot{y}_c}{\sqrt{x_c^2 + y_c^2}}\right) \cdot \frac{1}{x_c^2 + y_c^2 + z_c^2} \\ &= \dot{z}_c - z_c\frac{x_c\dot{x}_c + y_c\dot{y}_c}{x_c^2 + y_c^2} \cdot \frac{x_c^2 + y_c^2}{\|r_c\|^2\sqrt{x_c^2 + y_c^2}} \\ &= \frac{\dot{z}_c R - z_c(x\dot{x}_c + y\dot{y}_c)/R}{R^2 + z_c^2}, \qquad R = \sqrt{x_c^2 + y_c^2}\end{aligned} \tag{24}$$

When the target point with coordinates $r_c = [x_c, y_c, z_c]^T$ is projected onto the image plane according to the pinhole model. Camera's internal norm matrix K:

$$K = \begin{bmatrix} f_x & s & c_x \\ 0 & f_y & c_y \\ 0 & 0 & 1 \end{bmatrix} \tag{25}$$

Where: f_x, f_y are the horizontal/vertical focal lengths, s is the skew coefficient – a calibration parameter describing the degree of non-orthogonality between two pixel axes, and (c_x, c_y) is the image center. Projecting LOS onto an image plane:

$$[u \quad v \quad 1]^T = K \begin{bmatrix} \frac{x_c}{z_c} & \frac{y_c}{z_c} & 1 \end{bmatrix}^T \tag{26}$$

In projection matrix form:

$$\pi(r_c) = \begin{bmatrix} u \\ v \end{bmatrix} = \begin{bmatrix} f_x \frac{x_c}{z_c} + c_x & f_y \frac{y_c}{z_c} + c_y \end{bmatrix}^T \tag{27}$$

To calculate the image Jacobian (from 3D motion to pixel velocity), we take the derivative with respect to time to arrive at the pixel velocity expression:

$$[\dot{u} \quad \dot{v}]^T = J_{img}(r_c)\dot{r}_c \tag{28}$$

With: $$J_{img}(r_c) = \begin{bmatrix} \frac{\partial u}{\partial x} & \frac{\partial u}{\partial y} & \frac{\partial u}{\partial z} \\ \frac{\partial v}{\partial x} & \frac{\partial v}{\partial y} & \frac{\partial v}{\partial z} \end{bmatrix} = \begin{bmatrix} f_x \frac{1}{z_c} & 0 & -f_x \frac{x}{z_c^2} \\ 0 & f_y \frac{1}{z_c} & -f_y \frac{y}{z_c^2} \end{bmatrix} \tag{29}$$

The image Jacobian matrix $J_{img}(r_c)$ is locally invertible for all $z_c > 0$, ensuring that all posture and velocity changes map differentiably to pixel shifts. Therefore, the extended LOS model always has a unique and continuous solution when the background velocity variables are differentiable.

Lemma 1. *Let the standard pinhole projection with internal norm f_x, f_y (non-negative and non-zero) and a point in the camera frame $r_c = (x, y, z)^T$ with $z \neq 0$. The image Jacobian matrix is calculated according to r_c via Equation (29) satisfies the following properties:*

a) If $z \neq 0$ and $f_x f_y \neq 0$, then $rank(J_{img}(r_c)) = 2$ (full row-rank). Therefore, the mapping $r_c \mapsto p = (u, v)$ is a local submersion, and the Jacobian has a full row.

b) The nullspace of $J_{img}(r_c)$ is a one-dimensional space generated by the vector r_c/z, i.e.:

$$ker\, J_{img}(r_c) = span\left\{ \left[\frac{x}{z}, \frac{y}{z}, 1\right]^T \right\} \tag{30}$$

c) Since $rank = 2$, there exists a Moore–Penrose pseudo-inverse row (right pseudo-inverse) for J_{img}:

$$J_{img}^{+} = J_{img}^{T}(J_{img}J_{img}^{T}) - 1 \tag{31}$$

and every pixel velocity vector $\dot{p} = [\dot{u}, \dot{v}]^T$ has a family of 3D velocity solutions $\dot{r}_c$ in the form

$$\dot{r}_c = J_{img}^{+}\dot{p} + \frac{\lambda r_c}{z}, \qquad \lambda \in R \tag{32}$$

d) Consequence according to the implicit function theorem: If z is kept fixed, then the mapping $(x, y) \mapsto (u, v)$ is locally invertible (has an invertible 2×2 Jacobian matrix), and it is possible to solve locally $(x, y) = \Phi(u, v; z)$.

Proof:

a) Consider the columns of $J_{img}(r_c)$:

$$c_1 = \begin{bmatrix} \frac{f_x}{z}, & 0 \end{bmatrix}^T; c_2 = \begin{bmatrix} 0, & \frac{f_y}{z} \end{bmatrix}^T; c_3 = \begin{bmatrix} -\frac{f_x x}{z^2}, & -\frac{f_y y}{z^2} \end{bmatrix}^T \tag{33}$$

Since $f_x \neq 0$, $f_y \neq 0$ and $z \neq 0$, vectors c_1 and c_2 are linearly independent (c_1 has a positive component in row 1, c_2 has a positive component in row 2, and the two vectors are not proportional.

Therefore, the row (or column) of the matrix has rank at least 2; since the matrix only has 2 rows, $\mathrm{rank}(J_{img}) = 2$.

b) Find $\dot{r}_c = [v_1, v_2, v_3]^T$ such that $J_{img}\dot{r}_c = 0$. From two rows:

$$\begin{gathered} \frac{f_x}{z}v_1 - \frac{f_x x}{z^2}v_3 = 0 \Rightarrow v_1 = \frac{x}{z}v_3 \\ \frac{f_y}{z}v_2 - \frac{f_y y}{z^2}v_3 = 0 \Rightarrow v_2 = \frac{y}{z}v_3 \end{gathered} \tag{34}$$

Therefore, all solutions have the form $v_3\left[\frac{x}{z}, \frac{y}{z}, 1\right]^T$. So, $\ker J_{img}(r_c) = \mathrm{span}\left\{\left[\frac{x}{z}, \frac{y}{z}, 1\right]^T\right\}$.

c) When rank $= 2$, the matrix $J_{img}J_{img}^T$ is invertible (2×2) and the Moore–Penrose pseudo-inverse definition as stated is valid. Every solution $\dot{r}_c$ of $J_{img}\dot{r}_c = \dot{p}$ is written generally as pseudo-inverse plus the nullspace free component, leading to the given expression.

d) If z is kept fixed, the submatrix $\partial(u,v)/\partial(x,y) = \mathrm{diag}(f_x/z,\ f_y/z)$ is diagonal with non-zero elements; therefore, it is 2x2 invertible. Thus, by the implicit function theorem, x, y can be solved locally as a function of u, v, and the parameter z.

The lemma has been proved.

■

2.3. Relation to image plane coordinates

If the camera moves, it has a linear velocity v_c of the camera within the camera frame, and ω_c is the angular velocity of the camera within the camera frame. These two movements will cause the pixels to change according to the following pattern:

$$\dot{r}_c = -\omega_c \times r_c - v_c \tag{35}$$

Thus, rotating the camera causes the entire image to spin around the center; when the camera is moved forward, the entire image slides in the same direction as the movement.

Instead of (30), the change of u, v over time due to camera velocity $\xi_c = [v_c,\ \omega_c]$:

$$[\dot{u} \quad \dot{v}]^T = J_{img}(r_c)(-\omega_c \times r_c - v_c) \tag{36}$$

From this point, every change in posture and background velocity maps differentially to a shift in the image center, which is the photographic representation of the dynamic LOS angle.

Lemma 2. *Assume the carrier has a small horizontal velocity component $v_\perp$ (perpendicular to LOS) compared to the observation distance r, and the line of sight deviation angle α satisfies $|\ \alpha\ | < 5°$. Then*

$$\dot{\alpha} \approx v_\perp / r \tag{37}$$

With an error of the quadratic approximation with respect to α (specifically $O\left(\left(\frac{v_\perp t}{r}\right)^2\right)$ the results show that the angular interference (LOS) increases inversely proportional to the distance to the target and is therefore more severe at close range.

Proof:

Consider simple geometry: At time t after the base begins to move horizontally $v_\perp$ (the target is stationary), the horizontal component creates a small angle $\alpha(t)$ satisfying (38)

$$\tan\alpha\,(t) = \frac{v_\perp}{r}t \Rightarrow \dot{\alpha} = \frac{v_\perp}{r}\cos^2\alpha \tag{38}$$

With a small angle ($\alpha < 5°$): $\quad \cos^2\alpha = 1 - O(\alpha^2) \approx 1 \quad (39)$

So that: $\quad \dot{\alpha} \approx v_\perp / r \quad (40)$

and the error is approximately proportional to α^2. Integrate (40) to get $\alpha \approx \frac{v_\perp t}{r}$, then we get the secondary error $O\left(\left(\frac{v_{\perp}t}{r}\right)^2\right)$.

The lemma has been proved.

■

3. SIMULATION ANALYSIS AND COMMENTARY

3.1. Simulation scenarios

Assume an electro-optical observatory is installed on the CV-01 ship [3]. Consider the perpendicular velocity component LOS $v_{\perp}$. The research calculates for two typical combat ranges: r = 300 m and r = 500 m; the base speeds considered are: 0.5÷5.0 m/s.

- Rate of change of LOS angle (rad/s): $\dot{\alpha} \approx v_{\perp}/r$; $\Delta\alpha = \dot{\alpha} \cdot \tau$ (rad).
- Pixel shift: $\Delta px = \Delta\alpha \cdot f_{px}$ (px).

3.2. Simulation results

The table below shows: Velocity v (m/s), angular velocity LOS (deg/s), $\Delta\alpha$ (deg), and Δpx at times 1s, 3s, and 5s. (Note that Δpx = ($\Delta\alpha$ in rad)·4000). All numerical values were generated directly from MATLAB scripts using the analytical expressions.

a) Case 1: All velocities are perpendicular to LOS, $v_{\perp} = v$

Table 1. *Simulation at a distance of $r = 300$ m.*

v (m/s)	$\dot{\alpha}$ (deg/s)	$\Delta\alpha$ @1s (deg)	$\Delta\alpha$ @3s (deg)	$\Delta\alpha$ @5s (deg)	Δpx @1s (px)	Δpx @3s (px)	Δpx @5s (px)
0.5	0.09549	0.09549	0.28648	0.47747	6.67	20.0	33.33
1.0	0.19099	0.19099	0.57296	0.95493	13.33	40.0	66.67
2.0	0.38197	0.38197	1.14592	1.90986	26.67	80.0	133.33
3.0	0.57296	0.57296	1.71887	2.86479	40.00	120.0	200.0
4.0	0.76394	0.76394	2.29183	3.81972	53.33	160.0	266.67
5.0	0.95496	0.95496	2.86488	4.77479	66.67	200.0	333.33

Table 2. *Simulation at a distance of $r = 500$ m.*

v (m/s)	$\dot{\alpha}$ (deg/s)	$\Delta\alpha$ @1s (deg)	$\Delta\alpha$ @3s (deg)	$\Delta\alpha$ @5s (deg)	Δpx @1s (px)	Δpx @3s (px)	Δpx @5s (px)
0.5	0.05728	0.05728	0.17185	0.28646	4.0	12.0	20.0
1.0	0.11457	0.11457	0.34370	0.57283	8.0	24.0	40.0
2.0	0.22918	0.22918	0.68755	1.14596	16.0	48.0	80.0
3.0	0.34378	0.34378	1.03133	1.71887	24.0	72.0	120.0
4.0	0.45837	0.45837	1.37510	2.29183	32.0	96.0	160.0
5.0	0.57296	0.57296	1.71887	2.86479	40.0	120.0	200.0

Remark 1. If the entire ship velocity is perpendicular to the LOS (which is very rare), then at $v = 5\ m/s$ and $r = 300\ m$, after 3 seconds, we have ~200 px deviation - an extremely large level, which will certainly lead to loss of traction.

b) Case 2 (Real-life scenario): The ship has an axial alignment and a small angle of deviation ($v = 5\ m/s, \delta = 1°, 2°, 3°$). We calculate $v_{\perp} = v\sin\delta$ with v = 5 m/s.

Table 3. *Simulation with $v = 5$ m/s.*

r (m)	δ (°)	$v_{\perp}$ (m/s)	$\dot{\alpha}$ (deg/s)	$\Delta\alpha$ @1s (deg)	$\Delta\alpha$ @3s (deg)	$\Delta\alpha$ @5s (deg)	Δpx @1s (px)	Δpx @3s (px)	Δpx @5s (px)
300	1	0.0873	0.01667	0.01667	0.05000	0.08333	1.16	3.49	5.82
300	2	0.1745	0.03333	0.03333	0.09998	0.16663	2.33	6.98	11.63
300	3	0.2617	0.04999	0.04999	0.14996	0.24994	3.49	10.47	17.49
500	1	0.0873	0.01000	0.01000	0.03000	0.05000	0.93	2.79	4.65
500	2	0.1745	0.02000	0.02000	0.05999	0.09998	1.40	4.19	6.98
500	3	0.2617	0.02999	0.02999	0.08996	0.14993	2.09	6.28	10.47

Remark 2. With $v = 5\,m/s$ and a small directional error of 1÷3°, after 3 seconds we get a low pixel shift - with $\delta \leq 1°$ it is extremely small (< 4 px @$r = 300$), $\delta = 3°$ causes ~10 px @$r = 300$ in 3 seconds. The velocity threshold can be determined based on the pixel tolerance target and the evaluation duration τ.

4. TEST RESULTS

The EO/IR camera used in the experiment had a resolution of 1920×1080 pixels and was rigidly mounted on the pan-tilt platform together with the IMU sensor. Pixel drift was estimated by tracking the image-center deviation frame-by-frame from recorded video sequences. GPS measurements were used to estimate the carrier trajectory and approximate observation distance during the sea trial with level 2 waves. The ship's position was measured by GPS, marked at 8 points in 2 trials. The camera's aiming direction was maintained along with the ship's direction. When the ship was heading straight towards the target, the image center was stable with a deviation of < 2 px, consistent with simulation results and the $v_{\perp} \approx 0$ characteristic. However, when the ship deviated by 2÷4°, the pixel shifted sharply with an amplitude of 8÷12 px according to the wave period and the phase of the direction shift. This variation is consistent with the $v_{\perp}/r$ model and confirms the structured nature of LOS interference rather than random interference. Experimental results confirm the correctness of the LOS dynamic model and demonstrate the necessity of the feedforward compensation branch from IMU/INS.

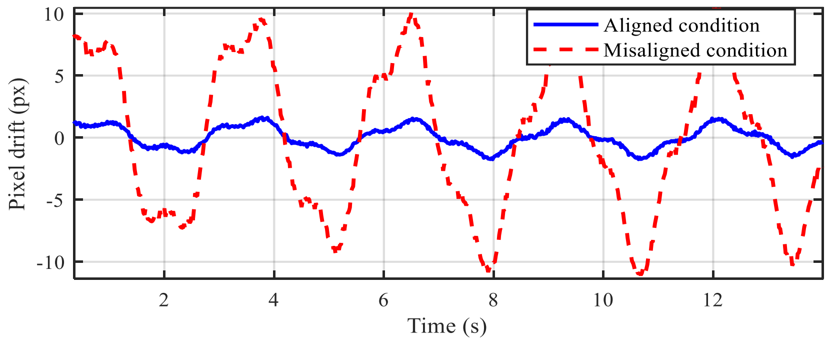

Figure 1. *Measured pixel drift under aligned and misaligned operating conditions.*

To further illustrate the LOS disturbance behavior, Figure 1 presents the measured pixel drift under aligned and misaligned operating conditions. When the vessel remained approximately aligned with the target direction, the image-center deviation stayed within approximately ±2 px. In contrast, heading misalignment produced significantly larger oscillatory pixel drift, with amplitudes approaching 8–12 px.

5. CONCLUSIONS

This paper constructed a first-order geometric-kinematic LOS model in the coordinate system of a camera mounted on the pan-tilt platform of the CV-01 vessel, including the influence of attitude and carrier velocity. Analysis results showed that although the CV-01's speed was low (≤ 5 m/s), the horizontal velocity component $v_{\perp}$ generated by the misalignment δ could still cause significant LOS deviation, especially at a distance of 300 m. With $\delta \geq 2 \div 3°$, $v_{\perp}$ and v close to 5 m/s, Δpx could reach 10 px in just a few seconds. Conversely, when the vessel was axially oriented towards the target ($\delta \approx 0°$), LOS interference was very small and did not affect image tracking quality. The study indicated that the danger zone was $r < 350\ m$ and $v_{\perp} > 2.5\ m/s$, with pixel drift exceeding 10 px in just 3 seconds. Based on simulations and analysis, this paper recommends considering the deployment of a feedforward compensation branch from the IMU/INS in combination with a modern control architecture such as LQR/LQG to improve the suppression of LOS interference, especially during rapid changes of direction or maneuvers.

REFERENCES

[1]. Vu Quoc Huy, *"Research and synthesize an automatic target tracking system controlling observatory in mobile vehicles"*, Dissertation, Academy of Military Science and Technology, VN, (2017).

[2]. Vu Quoc Huy, *"Euler-Lagrange Equation of optical electronics observator in mobile vehicle"*, Special Issue. CAPITI, Journal of Military Science and Technology, pp. 70-78, (2019).

[3]. Trương Tất Thuấn, Lê Việt Hồng, & Vũ Quốc Huy, *"Research on the motion rules of the pan-tilt electromechanical system in the launch platform stabilization system on ships"*, Journal of Military Science and Technology, (CAPITI), pp. 49–55, (2024). DOI: https://doi.org/10.54939/1859-1043.j.mst.CAPITI.2024.49-55

[4]. Larry A. Stockum and George R. Carroll, *"Precision Stabilized Platforms For Shipboard Electro-Optical Systems"*, Proc. SPIE 0493, Optical Platforms, (1984). DOI: https://doi.org/10.1117/12.943843

[5]. S. Skogestad and I. Postlethwaite, Multivariable Feedback Control: Analysis and Design, 2nd ed., Wiley, (2005). ISBN 978-0470011683

[6]. Armel Crétual, François Chaumette, *"Dynamic Stabilization of a Pan and Tilt Camera for Submarine Image Visualization"*, Computer Vision and Image Understanding, Vol. 79, Iss. 1, pp. 47-65, (2000). DOI: https://doi.org/10.1006/cviu.2000.0849

[7]. S. Singh, R. Marathe, A. Kumar, and R. Kumar, *"Sliding mode control based line-of-sight (LOS) stabilization of electro-optical sighting system"*, 2016 IEEE 1st International Conference on Power Electronics, Intelligent Control and Energy Systems (ICPEICES), Delhi, India, pp. 1-6, (2016). DOI: 10.1109/ICPEICES.2016.7853071

[8]. Gao, Q., Sun, Q., Qu, F., Wang, J., Han, X., & Zhao, J., *"Line-of-sight rate modeling and error analysis of inertial stabilized platforms by coordinate transformation"*, Proceedings of the Institution of Mechanical Engineers, Part B: Journal of Engineering Manufacture, 233, pp. 1317 - 1322, (2019).

[9]. Baskin, M., & Leblebicioğlu, M. K., *"Robust control for line-of-sight stabilization of a two-axis gimbal system"*, Turkish Journal of Electrical Engineering and Computer Sciences, 25 (5), pp. 3839-3853, (2017). DOI: https://doi.org/10.3906/elk-1606-435

[10]. Singh, A., Thakur, R., & Chatterjee, D. S., *"Design and Optimal Control of Line of Sight Stabilization of Moving Target"*, IOSR Journal of Electrical and Electronics Engineering, 9 (5), pp. 27–32, (2014). DOI: https://doi.org/10.9790/1676-09532732

[11]. Xia, Y., Bao, Q., Liu, Z., *"A New Disturbance Feedforward Control Method for Electro-Optical Tracking System Line-Of-Sight Stabilization on Moving Platform"*, Sensors, Vol. 18, pp. 4350, (2018). DOI: https://doi.org/10.3390/s18124350

[12]. Lan, L., Jiang, W., Hua, F., *"Research on the Line of Sight Stabilization Control Technology of Optronic Mast under High Oceanic Condition and Big Swaying Movement of Platform"*, Sensors, Vol. 23, pp. 3182, (2023). DOI: https://doi.org/10.3390/s23063182

[13]. Yingfeng Ji, Ronald A. Perez, Ryoichi S. Amano, *"Modeling and Control of Underwater Pan/Tilt Camera Tracking System: Geometry Modeling and Tracking Control"*, ASME International Mechanical Engineering Congress and Exposition, IMECE2009-10517, pp. 855-863, (2010).
[14]. Christian R. Sonnenburg, *"Modeling, Identification, and Control of an Unmanned Surface Vehicle"*, Dissertation, December 7th, Blacksburg, Virginia, (2012).

TÓM TẮT

Động học góc đường ngắm và sai lệch tâm ảnh của đài quan sát trên phương tiện cơ động có xét ảnh hưởng vận tốc và tư thế

Bài báo phân tích sự hình thành nhiễu đường ngắm (Line-Of-Sight, LOS) trên hệ thống EO/IR do chuyển động nền mang thông qua mô hình động học ba hệ tọa độ và chiếu hình pinhole. Từ các công thức biểu diễn, bài báo làm rõ ảnh hưởng của vận tốc ngang $v_\perp$ và sai lệch góc hướng δ đến tốc độ xoay LOS và mức dịch chuyển điểm ảnh (pixel drift). Kết quả mô phỏng cho thấy nhiễu rất nhỏ khi nền mang hướng thẳng vào mục tiêu, nhưng tăng đáng kể khi tồn tại thành phần vận tốc ngang, đặc biệt trong các pha đổi hướng hoặc duy trì mục tiêu ở vị trí lệch camera. Trên cơ sở đó, bài báo gợi ý hướng tiếp cận điều khiển phù hợp trong tương lai. Các kết quả thu được cung cấp cơ sở định lượng hữu ích cho thiết kế, vận hành và tối ưu hóa hệ bám ảnh EO/IR trong điều kiện nền mang cơ động.

Từ khoá: Động lực học đường ngắm; Ổn định quang điện; Động học hình học; Độ lệch mặt phẳng ảnh; Nền tảng di động.